Refractive index determination of buffer solutions from visible to near-infrared spectral range for multispectral quantitative phase imaging using a calibrated Abbe refractometer

Álvaro Barroso*, Rohan Radhakrishnan, Steffi Ketelhut, Jürgen Schnekenburger, Björn Kemper
Biomedical Technology Center of the Medical Faculty, University of Muenster,
Mendelstr. 17, D-48149, Germany;

ABSTRACT

Information about the refractive index difference between a biological material and its surrounding medium is of key importance in various research fields in biophotonics. However, the optical properties of many physiological buffer solutions are not well characterized over a broad spectral range. In this study, we measure the refractive index of mainly transparent liquids commonly used for live cell imaging and tissue embedding in the wavelength range from 500 nm to 1100 nm utilizing a modified and calibrated Abbe refractometer. The presented approach for obtaining multi-spectral refractive index data builds the basis to retrieve the dispersion coefficients of various physiological buffer solutions.

Keywords: hyperspectral imaging, refractive index, dispersion, refractometer, buffer solution

1. INTRODUCTION

The refractive index (RI) difference between a biological material and its surrounding medium is of key importance in various research fields in biophotonics, like in high-resolution optical coherence tomography (OCT), quantitative phase imaging (QPI) or optical tweezers (OT).[1–6] Depending on specimen and experimental conditions, like, e.g., temperature, required osmotic pressure or oxygen concentration, biological samples have to be prepared in different buffer solutions. However, the optical properties of such buffer solutions are often unknown for a broad spectral range, as, for example, it is required for hyperspectral imaging approaches. Since its invention in 1869 by Ernst Abbe, the Abbe refractometer has been one of the most employed instruments to measure the RI of liquids. The typical use of compensating prisms in Abbe refractometers provides the determination of the RI of the liquid under test for a specific wavelength, typically sodium-yellow line (λ_D = 589 nm). In order to overcome this limitation, various approaches for refractometry and interferometry-based methods have been successfully applied to determine the refractive index of liquids over a broad spectral range.[7–12] Most studies have been focused on water and organic compounds. However, almost no information about the dispersion of the refractive index of physiological buffer solutions over a broad spectral range is available.

In this study, we present a method for refractive index retrieval from the visible to the near infrared regime that is suitable for the analysis of buffer solutions commonly applied in live cell imaging. A standard Abbe refractometer was slightly modified and combined with two digital sensors that cover the visible and near-infrared spectral range. As light source, a continuously tuneable supercontinuum laser was used, providing optical radiation in the range from 500 nm to 1100 nm. The dispersion of the compensating prism, which is present in most Abbe refractometers, was considered by an adapted calibration procedure. The presented concept for obtaining refractive index data in the wavelength range from 500 nm and 1100 nm builds the basis for the retrieval of the dispersion coefficients of various physiological buffer solution.

*alvaro.barroso@uni-muenster.de;

Quantitative Phase Imaging V, edited by Gabriel Popescu, YongKeun Park, Proc. of SPIE Vol. 10887, 1088729

2. CONCEPT FOR DETERMINATION OF REFRACTIVE INDEX OF LIQUIDS

2.1 Operating principle of the utilized Abbe refractometer

A schematic of the optical system of a conventional Abbe refractometer is depicted in Figure 1(a). In a refractometer, based on Abbe's concept, the medium whose refractive index n_m has to be measured is confined between two prisms. The first prism is known as the *illuminating prism.* It features a rough surface at the prism-medium interface. The matted surface creates diffusely scattered light that enters the liquid layer at all angles. The second prism is known as the *measuring prism* or *Abbe prism* (A-prism) and it is typically made of glass with a refractive index $n_P \approx 1.75$. The normal to the emergence face of the A-prism is known as the axis of *alidade*. A telescope is used to detect the refracted light by the A-prism.

The operating principle of Abbe refractometers is based on critical refraction. Since the refractive index of the medium n_m is lower than the refractive index of the prism n_P (see Fig. 1(a)), the illumination rays that incidents the medium-prism interface under arbitrary angles α_1 are refracted by the A-prism at angles $\alpha'_1 < \alpha_c$, where α_c is the cutoff angle or the *critical angle*. In this way, the light rays transmitted through the A-prism are subsequently refracted at the prism-air interface at angles $\alpha'_2 > \gamma$, where γ is denoted here as the *critical emergence angle*. Figures 1(b)-(c) show the traces of two light rays with incidence angle $\alpha_1 = 40°$ and $\alpha_1 = 90°$ that propagates from a medium with $n_m = 1.33$ and A-prism with $n_P = 1.75$. For monochromatic light, a sharp edge separating a bright from a dark field, also known as the *critical edge*, is imaged on the crosshairs under appropriate orientation of the alidade, as shown in Fig. 1(a). For measuring the refractive index of the test liquid, the A-prism is rotated until the critical edge is centered at the crosshairs. The value of refractive index is measured at a sector scale that is attached rigidly to the rotating A-prism. If the source of light is non-monochromatic, the light is dispersed by the combined effect of refraction at the medium-prism and prism-air interface, resulting in a color gradient at a crosshairs instead of a dark-bright boundary. To account for this effect, Abbe refractometers typically feature a couple of Amici prism or compensating prisms (C-prisms) in order to produce a colorless and sharp edge.

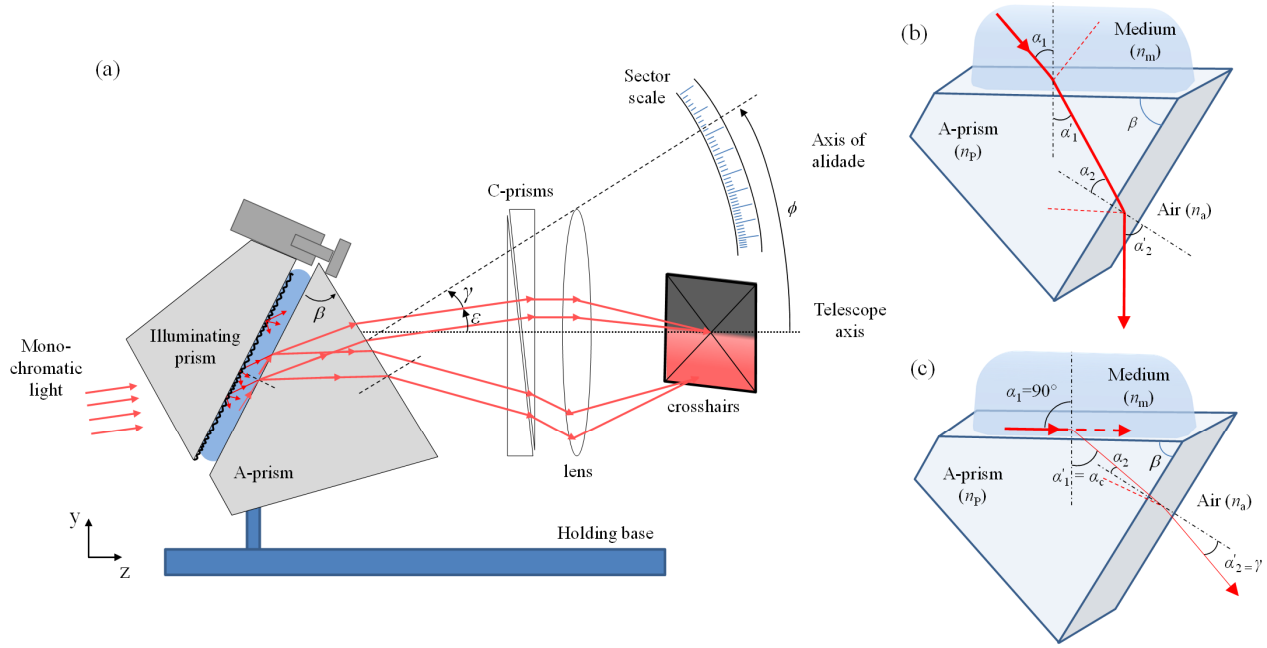

Figure 1. (a) Typical optical concept of an Abbe refractometer[13]. (b) –(c) Simulation of the refraction of a light ray with incidence angle (b) $\alpha_1 = 40°$ and (c) $\alpha_1 = 90°$. The ray traces were calculated utilizing a computational toolbox[14] and using as refractive indices for the medium and the A-prism $n_m = 1.33$ and $n_P = 1.75$, respectively. The red dashed lines represent the reflected rays and the continuous red lines represent the refracted rays. The thickness of the red lines correlates with the optical power of the light rays. ϕ: Angle between alidade and telescope axes; ε: angle of deviation due to the *C*-prisms; γ: critical emergence angle.

2.2 Measurement of the refractive index for multiple light wavelengths

C-prisms are designed for a particular wavelength at which light is not deviated regardless the relative orientation of the prisms, usually for the sodium-yellow line (λ_D = 589.3 nm). Thus, when using a monochromatic light source with this calibration wavelength, the value of the refractive index can be obtained independently of the C-prism configuration. However, if the monochromatic light is of variable wavelength, the measured value at the sector scale is inaccurate, and a calibration procedure has to be performed.[13]

According to Snell's law of refraction, an incoming ray from the matted surface of the illuminating prism with incident angle α_1 respect the normal to the medium/A-prism interface is refracted by an angle α'_1:

$$n_m \sin\alpha_1 = n_P \sin\alpha'_1 . \tag{1}$$

At the prism-air interface a second refraction occurs:

$$n_P \sin\alpha_2 = n_a \sin\alpha'_2 \tag{2}$$

where α_2 and α'_2 are the incident and refracted angles, respectively, with respect to the normal to the prism-air interface, and n_a is the refractive index of air.

The prism angle or apex angle β is related with α'_1 and α_2 and by:

$$\beta = \alpha'_1 + \alpha_2 . \tag{3}$$

In this way, $\sin\alpha'_1$ can be expressed in terms of β and α_2 as:

$$\sin\alpha'_1 = \sin(\beta - \alpha_2) = \sin\beta\cos\alpha_2 - \cos\beta\sin\alpha_2 . \tag{4}$$

Next, inserting Equation (4) into Equation (1), and using the Pythagorean trigonometric identity yields:

$$n_m \sin\alpha_1 = n_P\left(\sin\beta\sqrt{1-\sin^2\alpha_2} - \cos\beta\sin\alpha_2\right). \tag{5}$$

The relation between the refractive index n_m of the sample as a function of the minimum deviation angle, i.e., for α_1=90°, can be obtained by inserting Equation (2) into Equation (5):

$$n_m = \sin\beta\sqrt{n_P^2 - (n_a\sin\gamma)^2} - n_a\cos\beta\sin\gamma . \tag{6}$$

For the specific case that the C-prisms act as a plane-parallel plate, the C-prism do not deviate the light rays (ε = 0) and the critical emergence angle is equal to the angle between the alidade and telescope axes ($\gamma = \phi$). This configuration is set when the C-prism are rotated either 90° or 270° with respect to each other, i.e., at the reading -30 or 30 on the drum scale of the C-prisms. Therefore, by measuring the angle between the alidade and the telescope axes, the true refractive index value n_m of the medium for each wavelength can be calculated:

$$n_m(\lambda) = \sin\beta\sqrt{n_P^2(\lambda) - \sin^2\phi(\lambda)} - \cos\beta\sin\phi(\lambda) , \tag{7}$$

where it has to be taken into account that the dispersion of the A-prism and the refractive index of air is assumed to be n_a≈1.0003. In case that the apex angle β and the dispersion of the refractive index of the A-prism are unknown, they can be obtained with a calibration procedure (see Section 3.1 and Section 3.2).

2.3 Experimental setup

Figure 2(a) shows a photo of the experimental setup. A commercial Abbe refractometer (WAY-2W, China) was mechanically fixed to an optical table and extended with two telescopes in such a way that the telescopes axes were aligned in parallel to the optical table. One telescope (the upper one in Figure 2(a)) was used for read out of the refractive index in the sector scale (Figure 2(b)), while the other one (the lower telescope in Figure 2(a)) was employed for adjusting the critical edge in the center of the crosshairs (Figure 2(c)). A relay lens was set at each telescope in order to image the corresponding image at a digital camera. Both, the sector scale and crosshairs images were acquired with two

standard industrial cameras, denoted as Camera 1 (DFK21BF04, The Imaging Source) and Camera 2 (DKM 23UP1300, The Imaging Source). As monochromatic light source, a continuously tunable supercontinuum laser with attached acousto-optic tunable filter (AOFT), was utilized, providing optical radiation in the range from 500 nm to 1100 nm (SuperK EXTREME EXR-15 or EXR-9 combined with a Super Select 4xVIS/IR or nIR1/-acousto-optic tunable filter (AOTF) and a single mode fiber SuperK FD7 PM, NKT Photonics A/S, Birkerød, Denmark). The drum scale of the compensating prisms was set to a plain-parallel configuration. Otherwise a calibration procedure was applied to consider the effect of the C-prisms.[13] The values provided by the manufacturer of the apex angle and refractive index of the A-prism at λ_D are β=58° and $n_p(\lambda_D)$ = 1.75518, respectively.[15] A goniometer was set at the rotating prisms in order to read the orientation of the alidade respect to the fixed telescope axis.

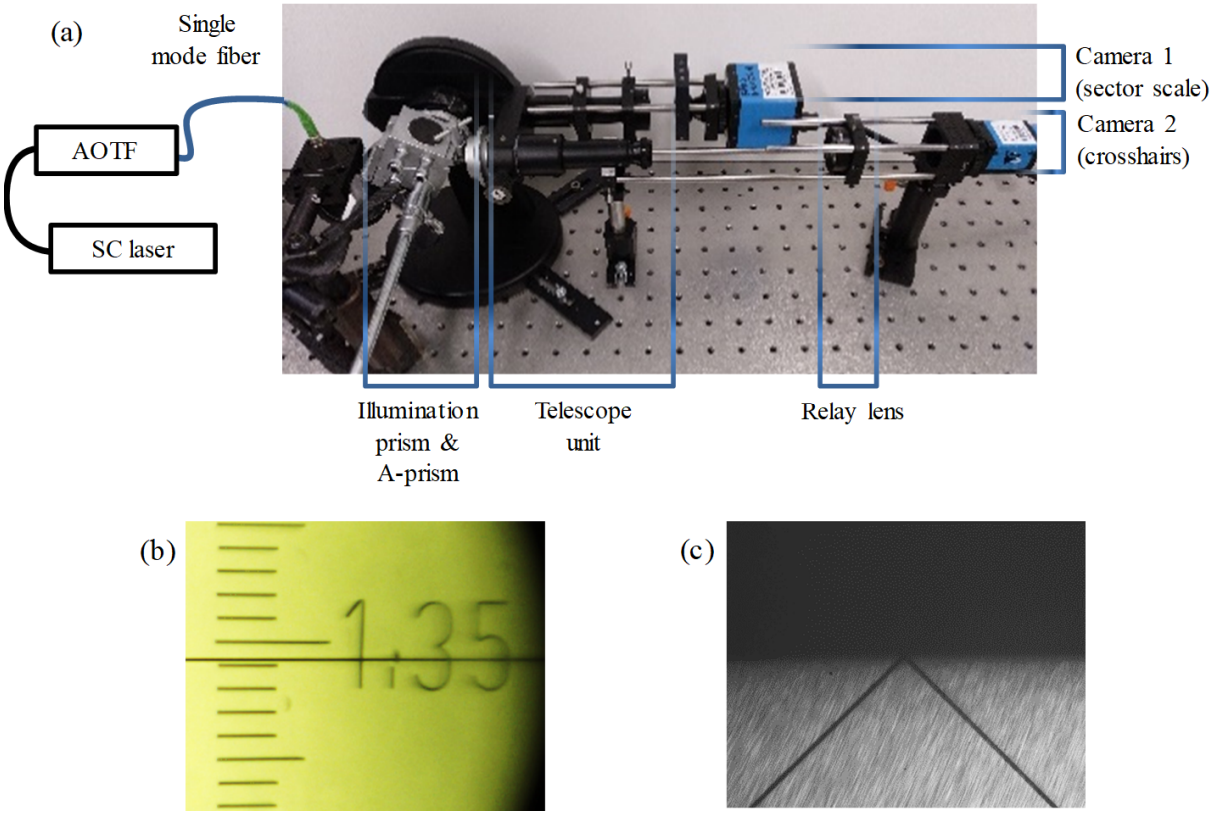

Figure 2. (a) Experimental setup and representative images of (b) the sector scale and (c) the crosshair of the Abbe refractometer. AOTF: Acousto-optic tunable filter, SC laser: supercontinuum laser.

3. CALIBRATION OF THE ABBE REFRACTOMETER

3.1 Calibration of apex angle of the A-prism and dispersion of refractive index of A-prism

As commented in Section 2.2, the reading value at the sector scale the value of the refractive index is incorrect when a different wavelength than the calibration wavelength is applied. Thus, a correction term Δn has to be determined and added to the reading value n_s at the sector scale in order to get the real value n_m:

$$n_m = n_S + \Delta n \quad . \tag{8}$$

For the calibration wavelength, Δn = 0, which gives a relation between the reading value n_s at the sector scale and the angle ϕ between the telescope and the alidade:

$$n_S = \sin\beta\sqrt{n_p^2(\lambda_D) - \sin^2\phi} - \cos\beta\sin\phi \quad . \tag{9}$$

In order to obtain the apex angle experimentally, one can measure the reading values n_s at the sector scale for different defined orientations of the alidade and subsequently fit Equation (9) to the measured data. Figure 4 plots the corresponding measured data points for our Abbe refractometer. Fitting Equation (9) to the data points as shown in Figure 3 yields an apex angle $\beta = (58.1 \pm 1.2)°$.

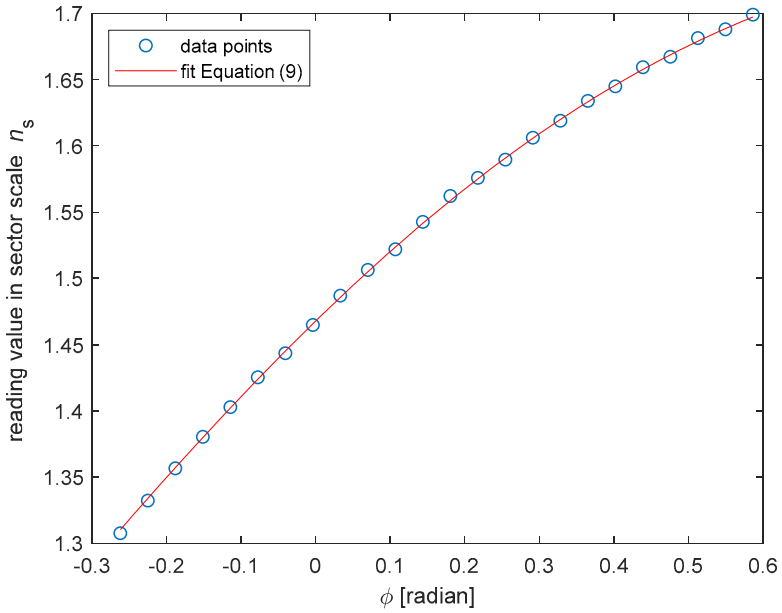

Figure 3. Reading values of the sector scale, n_s, as a function of the angle between alidade and telescope axes, ϕ, and the corresponding fitting of Equation (9) to the experimental data in order to determine the apex angle β of the measuring prism.

3.2 Calibration of dispersion of refractive index of the A-prism

The refractive index dispersion of the A-prism can be measured experimentally by using a test sample with a known refractive index. Solving Equation (7) for n_p yielts:

$$n_p(\lambda) = \sqrt{\left(\frac{n_m(\lambda) + \cos\beta \sin\phi(\lambda)}{\sin\beta}\right)^2 + \sin^2\phi(\lambda)} \qquad (10)$$

In order to characterize $n_p(\lambda)$, the angle between the alidade and telescope axes $\phi(\lambda)$ was determined using high-purity water (pure H_2O) as the test liquid, since its optical properties are well-characterized.[16] Measurements were performed from λ=500 nm to λ=1100 nm in steps of $\Delta\lambda$=1 nm. For each wavelength the angle $\phi(\lambda)$ was calculated by solving numerically Equation (9) using the measured n_s at the sector scale as input. Finally, Equation (10) was applied to obtain the dispersion of the refractive index of the A-prism using the values of the refractive index of water in the literature as reference.[16] The resulting values of $n_p(\lambda)$ are plotted in Figure 4 and fitted to the Cauchy's equation:

$$n^2 = C_0 + \frac{C_1}{\lambda^2} + \frac{C_2}{\lambda^4} + C_3\lambda^2 \qquad (11)$$

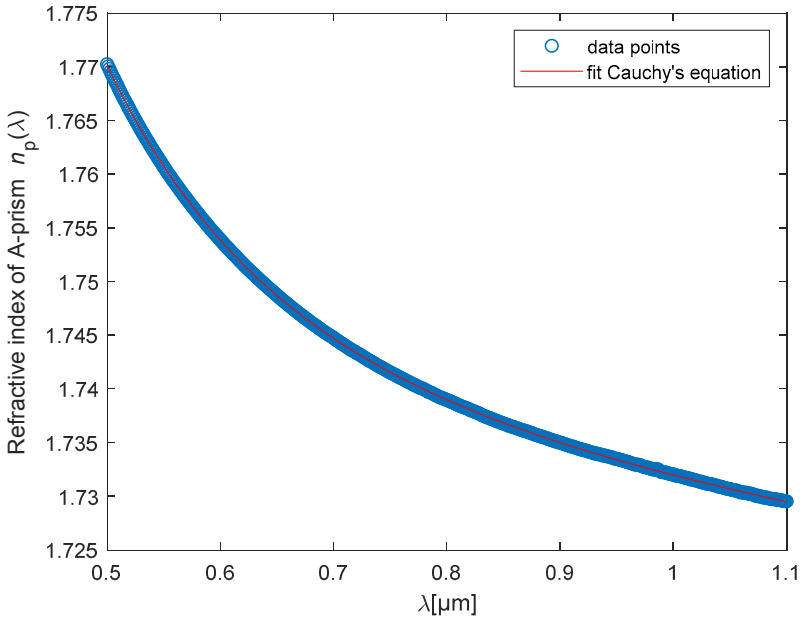

Figure 4. Refractive index dispersion of the measuring prism in the Abbe refractometer. The data points (blue dots) were obtained using high-purity water (pure H_2O) as reference liquid. The red line indicates the result of fitting Cauchy's equation (Eq. 11) to the experimentally obtained data points. The constants of Cauchy formula of the A-prism of our Abbe refractometer at a temperature of 22 °C are: C_0 = 1.7292 ± 0.0004, C_1 = 0.006213 ± 0.0004, C_2 = 0.00142 ± 0.00012, and C_3= -0.00008 ± 0.00002.

4. REFRACTIVE INDEX DETERMINATION OF PHYSIOLOGICAL BUFFER SOLUTIONS FROM VISIBLE TO NEAR-INFRARED SPECTRAL RANGE

The refractive index dispersion of typical physiological buffer solutions was analyzed:

- Dulbecco's Phosphate Buffered Saline (DPBS, Sigma-Aldrich);
- DPBS supplemented with 2mM Ethylenediaminetetraacetic acid (EDTA) and 0.5% bovine serum albumin (BSA);
- Dulbecco's Modified Eagle's Medium (DMEM, Sigma-Aldrich) supplemented with 2 mM glutamine, 1 mM sodium pyruvate, and 1% penicillin-streptomycin;
- DMEM (Sigma-Aldrich) supplemented with 10% fetal bovine serum (FBS), 2 mM glutamine, 1 mM sodium pyruvate, and 1% penicillin-streptomycin;
- 4-(2-hydroxyethyl)-1-piperazineethane-sulfonic acid (HEPES)-buffered DMEM (DMEM with 20 mM HEPES, 4 mM glutamine, 1mM sodium pyruvate, 10% FBS, 850mg/l $NaHCO_3$).

Measurements were performed in the spectral range from λ=500 nm to λ=1100 nm in steps of $\Delta\lambda$=1 nm at a temperature of 22°C. The determination of the refractive index for each wavelength was performed by applying Equation (7), previously obtaining the angle ϕ solving numerically Equation (9) using the measured n_s at the sector scale for each wavelength. The obtained results for the refractive index dispersion of the analyzed solutions are plotted in Figure 5. The constants that were obtained from fitting of the Cauchy's formula (Equation 11) to the experimental data are showed in Table 1.

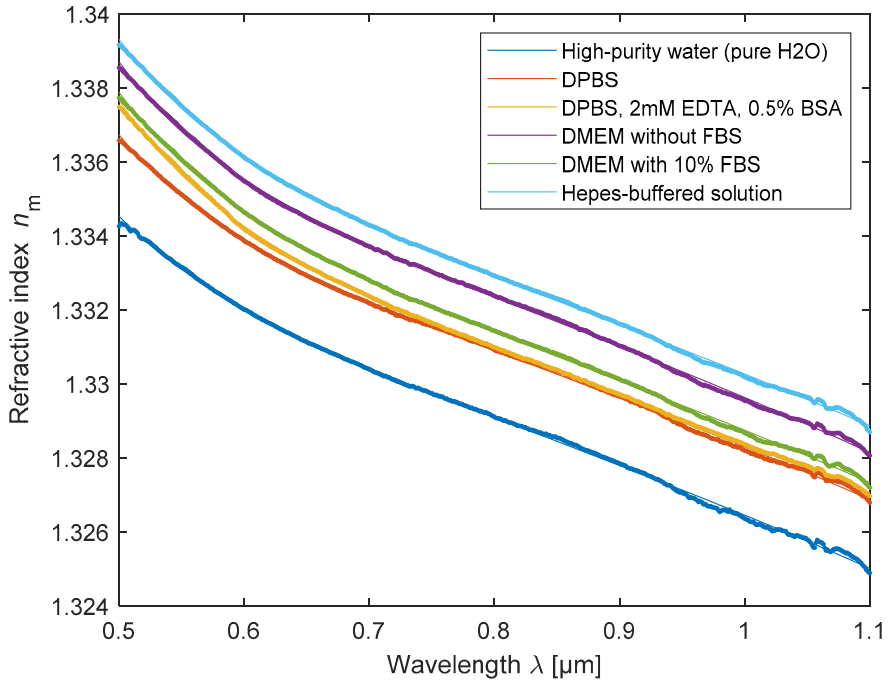

Figure 5. Refractive index dispersion retrieved in the spectral range from 500 to 1100 nm from measurements on different physiological buffer solutions at a temperature of 22°C.

Table 1. Constants of Cauchy's formula obtained by fitting of Eq. 11 to experimental the experimental data retrieved from of high-purity water, DPBS, DPBS with 2mM EDTA and 0.5% BSA, DMEM, DMEM with 10% FBS, and Hepes-buffered solution measured at a temperature of 22°C.

Medium	**C_0**	**C_1**	**C_2**	**C_3**
High-purity water (pure H_2O)	1.7765 ± 0.0012	-0.0002 ± 0.0006	0.0006 ± 0.0001	-0.0174 ± 0.0007
DPBS	1.7828 ± 0.0011	-0.0015 ± 0.0006	0.0009 ± 0.0001	-0.0179 ± 0.0006
DPBS, 2mM EDTA, 0.5% BSA	1.7810 ± 0.0009	-0.0010 ± 0.0005	0.0010 ± 0.0001	-0.0163 ± 0.0005
DMEM without FBS	1.7878 ± 0.0011	-0.0020 ± 0.0006	0.0011 ± 0.0001	-0.0188 ± 0.0006
DMEM with 10% FBS	1.7826 ± 0.0010	-0.0008 ± 0.0006	0.0009 ± 0.0001	-0.0171 ± 0.0006
Hepes-buffered solution	1.7862 ± 0.0010	-0.0006 ± 0.0005	0.0009 ± 0.0001	-0.0169 ± 0.0005

5. CONCLUSIONS

Information about the spectral refractive index variation of buffer solutions is essential in optical imaging of biological specimens, in particular for high-resolution imaging with optical coherence tomography, the correct evaluation of quantitative phase images of cell and tissues or for the calculation of the optical forces exerted in optical manipulation experiments. We thus have utilized a simple and robust concept for the retrieval of the index dispersion of semitransparent liquids using a modified and calibrated Abbe refractometer in combination with a supercontinuum laser as tunable light source and acquired experimental data for the refractive index dispersion of typical liquids commonly employed in the analysis of living cells and freshly dissected tissues. Our results pave the way to more extended studies on the dispersion coefficients of various physiological buffer solutions.

ACKNOWLEDGEMENTS

Financial support by the European Union (Horizon 2020 Project GALAHAD, no: 732613) and the state NRW Leitmarkt project "MicroPlastiCarrier" are gratefully acknowledged.

REFERENCES

[1] Park, Y. K., Depeursinge, C. and Popescu, G., "Quantitative phase imaging in biomedicine," Nat. Photonics **12**(10), 578–589 (2018).

[2] Kemper, B., Kosmeier, S., Langehanenberg, P., von Bally, G., Bredebusch, I., Domschke, W. and Schnekenburger, J., "Integral refractive index determination of living suspension cells by multifocus digital holographic phase contrast microscopy.," J. Biomed. Opt. **12**(5), 054009 (2007).

[3] Barroso, Á., Ketelhut, S., Heiduschka, P., Kastl, L., Schnekenburger, J. and Kemper, B., "Hyperspectral digital holographic microscopy approach for reduction of coherence induced disturbances in quantitative phase imaging of biological specimens," Proc. SPIE **10834**(Speckle 2018: VII International Conference on Speckle Metrology), 108340I (2018).

[4] Stevenson, D. J., Gunn-Moore, F. and Dholakia, K., "Light forces the pace: optical manipulation for biophotonics.," J. Biomed. Opt. **15**(4), 041503 (2010).

[5] Gao, D., Ding, W., Nieto-Vesperinas, M., Ding, X., Rahman, M., Zhang, T., Lim, C. T. and Qiu, C. W., "Optical manipulation from the microscale to the nanoscale: Fundamentals, advances and prospects," Light Sci. Appl. **6**(February) (2017).

[6] Barroso, Á., Woerdemann, M., Vollmer, A., Von Bally, G., Kemper, B. and Denz, C., "Three-dimensional exploration and mechano-biophysical analysis of the inner structure of living cells," Small **9**(6), 885–893 (2013).

[7] Kedenburg, S., Vieweg, M., Gissibl, T. and Giessen, H., "Linear refractive index and absorption measurements of nonlinear optical liquids in the visible and near-infrared spectral region," Opt. Mater. Express **2**(11), 1588 (2012).

[8] Lan, G., Gao, Y. and Zhang, X., "Measurement of chromatic dispersion of liquid in a wide spectral range based on liquid-prism surface plasmon resonance sensor," Sens. Bio-Sensing Res. **16**(September), 32–36 (2017).

[9] Rocha, A. C. P., Silva, J. R., Lima, S. M., Nunes, L. A. O. and Andrade, L. H. C., "Measurements of refractive indices and thermo-optical coefficients using a white-light Michelson interferometer," Appl. Opt. **55**(24), 6639 (2016).

[10] Stchakovsky, M., Battie, Y. and Naciri, A. E., "An original method to determine complex refractive index of liquids by spectroscopic ellipsometry and illustrated applications," Appl. Surf. Sci. **421**, 802–806 (2017).

[11] Sokolov, V. I., Savelyev, A. G., Bouznik, V. M., Igumnov, S. M., Khaydukov, E. V., Molchanova, S. I., Tuytuynov, A. A., Akhmanov, A. S. and Panchenko, V. Y., "Refractive index and dispersion of highly fluorinated acrylic monomers in the 1.5μm telecom wavelength region measured with a spectroscopic Abbe refractometer," Meas. Sci. Technol. **25**(7) (2014).

[12] Rheims, J., Köser, J. and Wriedt, T., "Refractive-index measurements in the near-IR using an Abbe refractometer," Mess. Sci. Technol. **8**, 601–605 (1997).

[13] Dodd, L. E., "Calibration of Abbe refractometer with compensating prisms, to measure refractive index for any wave length," Rev. Sci. Instrum. **2**(8), 466–501 (1931).

[14] Callegari, A., Mijalkov, M., Gököz, A. B. and Volpe, G., "Computational toolbox for optical tweezers in geometrical optics," J. Opt. Soc. Am. B **32**(5) (2014).

[15] "Specifications WYA-2W Abbe Refractometer.", <http://www.yiceyiqi.com/English/WYA-2W.html>.

[16] Daimon, M. and Masumura, A., "Measurement of the refractive index of distilled water from the near-infrared region to the ultraviolet region," Appl. Opt. **46**(18), 3811–3820 (2007).